Absorption of Transverse Spin Current in Ferromagnetic NiCu: Dominance of Bulk Dephasing over Spin-Flip Scattering

Youngmin Lim[1,(a)], Shuang Wu[1,(b)], David A. Smith[1,(c)], Christoph Klewe[2], Padraic Shafer[2], Satoru Emori[1,*]

1. Department of Physics, Virginia Tech, Blacksburg, Virginia 24060

2. Advanced Light Source, Lawrence Berkeley National Laboratory, Berkeley, California 94720

(a) current affiliation: Micron Technology, Boise, Idaho 83716

(b) current affiliation: Western Digital Corporation, San Jose, California 95119

(c) current affiliation: HRL Laboratories, Malibu, California 90265

* email: semori@vt.edu

In ferromagnetic metals, transverse spin currents are thought to be absorbed via dephasing – i.e., destructive interference of spins precessing about the strong exchange field. Yet, due to the ultrashort coherence length of ≈1 nm in typical ferromagnetic thin films, it is difficult to distinguish dephasing in the bulk from spin-flip scattering at the interface. Here, to assess which mechanism dominates, we examine transverse spin-current absorption in ferromagnetic NiCu alloy films with reduced exchange fields. We observe that the coherence length increases with decreasing Curie temperature, as weaker dephasing in the film bulk slows down spin absorption. Moreover, nonmagnetic Cu impurities do not diminish the efficiency of spin-transfer torque from the absorbed spin current. Our findings affirm that transverse spin current is predominantly absorbed by dephasing inside the nanometer-thick ferromagnetic metals, even with high impurity contents.

Spin currents underpin a variety of fundamental condensed-matter phenomena and technological applications [1–3], especially those based on magnetic materials. Of particular interest is coherent *transverse* spin current, where the flowing spins are uniformly polarized transverse to the magnetization. This spin current generates a spin-transfer torque that can switch a nanomagnetic memory or drive a GHz-range oscillator [4–6]. While spins may be carried by magnons [7] and phonons [8], they are often primarily carried by electrons in practical metallic multilayers incorporating ferromagnetic thin films. It is therefore crucial to understand the nanoscale transport of electron-mediated transverse spin current in ferromagnetic metals.

A spin current in any material ultimately becomes absorbed (loses coherence) within a finite length scale [1]. In ferromagnetic metals, transverse spin-current absorption can occur via *dephasing* [9–11], i.e., destructive interference of coherent spins that precess about the magnetic exchange field. The dephasing mechanism is illustrated in Fig. 1: The transverse electronic spins enter the ferromagnetic metal with a wide distribution of incident wavevectors; these spins traverse and precess about the magnetic exchange field at different rates, thereby averaging out the net transverse polarization (destroying the phase coherence) of the spin current within a finite length scale. Another possible mechanism of spin-current absorption is diffusive *spin-flip scattering* [12]. When electrons carrying the spin current are scattered, e.g., by impurities or an interface, the orientation of the propagating spins may be flipped to various orientations.

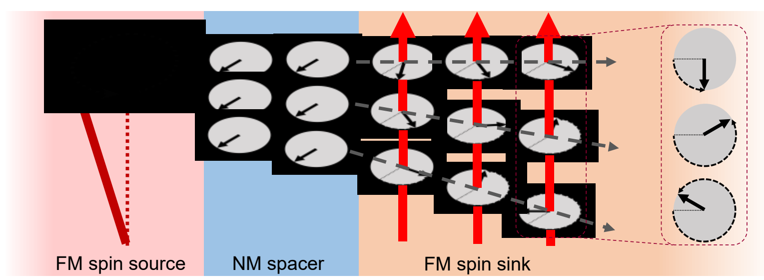

FIG. 1. Dephasing of a transverse spin current generated by FMR in the ferromagnetic (FM) spin source. The propagating spins are coherent in the normal metal (NM) spacer – as illustrated by the aligned black arrows – but they enter the spin sink with different incident wavevectors. In the FM spin sink, the spins precess about the ferromagnetic exchange field (red vertical arrows) by different amounts, thereby losing phase coherence.

Prior experiments [13] have quantified the absorption length scale – i.e., coherence length λ_c – of transverse spin current through ferromagnetic resonance (FMR) spin pumping [14]. These experiments indicate $\lambda_c \approx 1$ nm from the ferromagnetic film thickness where the measured spin absorption saturates. This ultrashort λ_c is presumably due to rapid dephasing [9–11] from the strong ferromagnetic exchange field of >> 100 T [15]. Hence, the conventional wisdom is that transverse spin current is absorbed via dephasing, rather than spin-flip scattering. However, $\lambda_c \approx$ 1 nm corresponds to a nominal film thickness of a few lattice parameters, likely just at the threshold of forming a continuous film layer. Spin-flip scattering at the "interface" could be significant for such ultrathin ferromagnets. Thus, a plausible alternative explanation for $\lambda_c \approx 1$ nm is that interfacial spin-flip scattering saturates at the ferromagnetic thickness of ≈1 nm. Spin-flip scattering by impurities in the ferromagnet bulk may also contribute to the short λ_c. Therefore, it generally remains a challenge to distinguish spin-flip scattering from spin dephasing.

In this Letter, we experimentally address the following fundamental question: Which mechanism – spin dephasing or spin-flip scattering – is responsible for the ultrashort coherence length λ_c of transverse spin current in ferromagnetic metals? By employing the FMR spin pumping protocol similar to Ref. [13], we quantify λ_c for ferromagnetic Ni films alloyed with nonmagnetic Cu that reduces the ferromagnetic exchange strength. Our hypothesis is that λ_c must increase with increasing nonmagnetic Cu impurity content, if dephasing in the bulk is dominant. On the other hand, if spin-flip scattering at the interface is dominant, λ_c is expected to remain mostly unchanged – or become shorter as the Cu impurities may enhance interfacial scattering. Similarly, λ_c should shorten if spin-flip scattering by the impurities in the bulk dominates. Thus, testing the above hypothesis permits us to confirm – or refute – the long-held notion that dephasing in the ferromagnet's bulk drives transverse spin-current absorption. It is also timely to examine basic spin transport in NiCu alloys, which have attracted attention for their reportedly sizable spin-orbit effects [16–18] that may hold promise for spintronic devices.

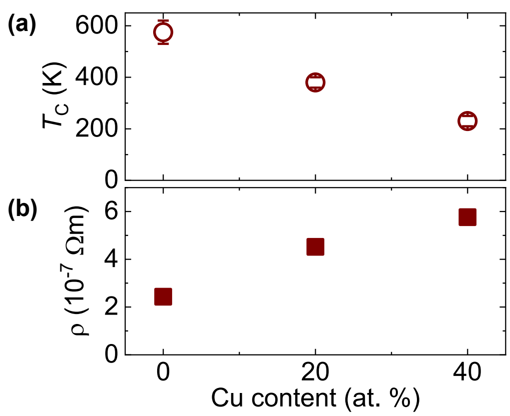

FIG. 2. Compositional dependence of (a) the Curie temperature T_C and (b) the electrical resistivity ρ of 10-nm-thick Ni(Cu) films.

Ni and Cu readily form homogeneous solid solutions, permitting continuous tuning of ferromagnetic exchange while maintaining the same face-centered cubic structure in NiCu alloys. Figure 2 summarizes the Curie temperatures T_C (the metric for the ferromagnetic exchange strength) and electrical resistivities ρ (the metric for the electronic scattering rate) of 10-nm-thick Ni, $Ni_{80}Cu_{20}$, and $Ni_{60}Cu_{40}$ films. We limit the maximum Cu content to 40 at.% to attain ferromagnetism close to room temperature, where our FMR spin pumping measurements were performed. The monotonic drop in T_C seen in Fig. 2(a) is consistent with prior reports [19,20] and verifies that the Cu impurities dilute the ferromagnetic exchange. The monotonic increase in ρ (Fig. 2(b)) confirms enhanced electronic scattering by the Cu impurities in the film bulk.

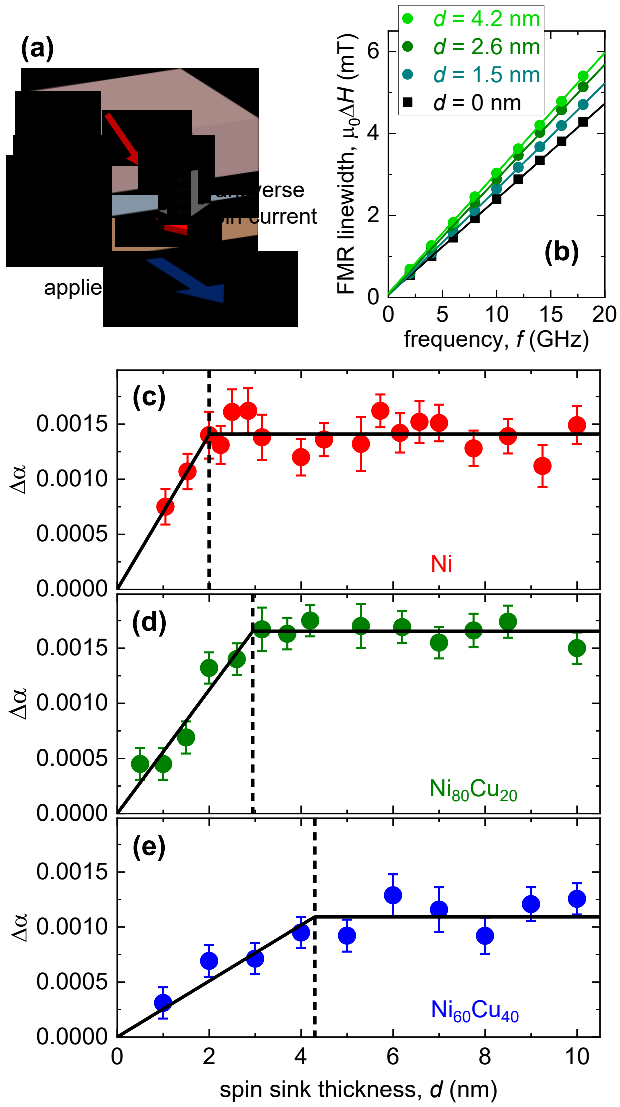

FIG. 3. (a) Illustration of FMR spin pumping with the NiFe spin source and the Ni(Cu) spin sink. (b) Frequency dependence of the FMR linewidth for different $Ni_{80}Cu_{20}$ spin sink thicknesses d. (c-e) Nonlocal damping enhancement $\Delta\alpha$ as a function of d, where the spin sink is (c) Ni, (d) $Ni_{80}Cu_{20}$, and (e) $Ni_{60}Cu_{40}$. The solid black lines indicate the fits with Eq. 1. The vertical dashed lines indicate the coherence length λ_c extracted from the fits.

To derive λ_c, we conducted FMR spin pumping measurements on film stacks Si-SiO_2(substrate)/Ti(3)/Cu(3)/$Ni_{80}Fe_{20}$(10)/Ag(5)/Ni(Cu)(0-10)/Ti(3), where Ni(Cu) denotes the Ni, $Ni_{80}Cu_{20}$, or $Ni_{60}Cu_{40}$ "spin sink." The Ti/Cu seed bilayer promotes narrow FMR linewidths (minimizing two-magnon scattering [21]) in the NiFe "spin source," crucial for straightforward spin pumping measurements. The Ag spacer suppresses direct magnetic coupling between the NiFe source and Ni(Cu) sink, such that spin transport from the source to the sink is mediated solely by electrons without complications from magnon interactions [22]. Ag is selected as the spacer, instead of the oft-used Cu, to reduce atomic intermixing at the spacer/Ni(Cu) interface.

In the spin pumping scheme (Fig. 3(a)), a microwave field from a coplanar waveguide excites FMR in the NiFe source, such that the magnetization oscillates about the in-plane applied bias magnetic field. FMR generates a coherent ac spin current polarized transverse to the oscillation axis. This spin current is pumped through the nonmagnetic Ag spacer and into the Ni(Cu) sink. Since the thickness of Ag here is much smaller than the spin diffusion length of ~100 nm [12,23], the coherent spin current propagates with negligible absorption in the spacer [14,24]. The polarization of the spin current is transverse to the magnetization of the Ni(Cu) sink, which is set by the applied field. The FMR condition of the Ni(Cu) layer is sufficiently far from that of the NiFe source, so Ni(Cu) serves as a passive sink that receives the spin current from the NiFe source.

Any spin-current absorption in the Ni(Cu) sink constitutes an additional loss of spin angular momentum, which manifests in an enhancement of Gilbert damping $\Delta\alpha$ in the NiFe source [14,25]. As shown in Fig. 3(b), the total measured Gilbert damping parameter α is obtained from the linear slope of the FMR linewidth ΔH plotted against the microwave frequency f, $\mu_0\Delta H = \mu_0\Delta H_0 + \frac{2\pi}{\gamma}\alpha f$, where $\mu_0\Delta H_0 < 0.1$ mT is the inhomogeneous linewidth broadening and $\frac{\gamma}{2\pi} = 29.8$ GHz/T is the gyromagnetic ratio for NiFe. By averaging samples from seven deposition runs, the baseline Gilbert damping parameter of NiFe/Ag without a Ni(Cu) sink is found to be $\alpha_0 = 0.00693 \pm 0.00014$, similar to other reports on NiFe thin films [26,27]. Figure 3(b) shows an increased slope of ΔH vs f with finite Ni(Cu) sink thickness. This observation signifies a nonlocal damping contribution, $\Delta\alpha = \alpha - \alpha_0$, due to spin absorption in the sink. Figure 3(c-e) summarizes the dependence of spin absorption, captured by $\Delta\alpha$, on spin-sink thickness d. For each d, an averaged α was obtained by measuring at least three separate sample pieces. The error bars for $\Delta\alpha$ are primarily from the scatter in α_0.

For each Ni(Cu) sink composition, $\Delta\alpha$ rises at small d and then saturates (Fig. 3(c-e)). This behavior is consistent with spin-current absorption within a finite depth in the sink, such that there is essentially no additional absorption at $d \gtrsim \lambda_c$. We quantify λ_c by fitting our experimental data of $\Delta\alpha$ vs d. One possible approach is to employ a modified drift-diffusion model [28–30], but this involves multiple free parameters (e.g., complex transmitted spin-mixing conductance [11,31]) that could produce overdetermined fits. Instead, we employ a simpler empirical fitting function employed by Bailey *et al.* [13,32,33] with only two parameters, i.e., λ_c and $\Delta\alpha_\mathrm{sat}$:

$$\Delta\alpha = \frac{\Delta\alpha_\mathrm{sat}}{\lambda_\mathrm{c}}\left(1 - H(d-\lambda_\mathrm{c})\right)d + \Delta\alpha_\mathrm{sat}H(d-\lambda_\mathrm{c}), \quad (1)$$

where $H(d-\lambda_\mathrm{c})$ is the Heaviside step function centered at $d = \lambda_\mathrm{c}$. From the resulting fits in Fig. 3(c-e), we note that $\Delta\alpha_\mathrm{sat}$ is slightly higher for the $Ni_{80}Cu_{20}$ sink whereas it is lower for $Ni_{60}Cu_{40}$. We attribute this variation in $\Delta\alpha_\mathrm{sat}$ to the different spin-mixing conductances that depend on the effective spin susceptibilities in these magnetic spin sinks [34–37]. We emphasize, however, that our focus here is on the length scale of transverse spin-current absorption, λ_c.

The values of λ_c from the fits with Eq. 1 are well over $\lambda_c = 1.2 \pm 0.1$ nm of $Ni_{80}Fe_{20}$ alloy from Ref. [13]. Specifically, we obtain $\lambda_c = 2.0 \pm 0.2$ nm for Ni, 3.0 ± 0.2 nm for $Ni_{80}Cu_{20}$, and 4.3 ± 0.5 nm for $Ni_{60}Cu_{40}$. These values exceed several atomic monolayers, strongly pointing to spin absorption in the *bulk* of the sink layer rather than at its interface.

We now consider which absorption mechanism in the bulk of Ni(Cu) is most consistent with the observation of longer λ_c with increasing Cu content. (i) *Dephasing due to the ferromagnetic exchange field* – A higher content of nonmagnetic Cu dilutes the ferromagnetic exchange field, hence slowing down the dephasing of the spin current. If dephasing dominates transverse spin absorption, λ_c should become longer with more Cu impurities. This scenario is indeed consistent with our observation. (ii) *Spin-flip scattering due to impurities* – A higher Cu impurity content enhances the momentum scattering of electrons (e.g., as evidenced by the increasing resistivity in Fig. 2(b) and a shorter mean free path [38]), which in turn increases the rate of spin-flips. The dominance of such spin-flip scattering (i.e., Elliott-Yafet spin relaxation expected in centrosymmetric metals at room temperature [1,39,40]) would yield *shorter* λ_c with more Cu impurities. This spin-flip-dominant scenario is contrary to our observation. We therefore deduce that dephasing, rather than spin-flip scattering, dominates the absorption of transverse spin current in Ni(Cu) examined here.

It is worth noting that the Dyakonov-Perel spin-relaxation mechanism can also result in longer λ_c with increasing scattering [1,41]. Yet, Dyakonov-Perel spin relaxation is another manifestation of dephasing, particularly from spins precessing about a spin-orbit field. Moreover, the dominance of Dyakonov-Perel spin relaxation would be surprising in centrosymmetric, polycrystalline Ni(Cu) at room temperature [39,40]. We therefore posit that the dephasing is primarily driven by the ferromagnetic exchange field.

To gain further insight into how λ_c scales with the diluted ferromagnetic exchange (i.e., decreasing T_C), we plot λ_c against the inverse of T_C for the Ni(Cu) compositions investigated in our work, along with $Ni_{80}Fe_{20}$ from Ref. [13]. Figure 4 illustrates the central finding of this study: λ_c scales inversely with the ferromagnetic exchange strength (represented by T_C). Again, the consistent explanation is that decreasing exchange – hence weaker dephasing – from the nonmagnetic Cu impurities enables the transverse spin current to remain coherent over a distance well above ≈1 nm. Our finding indicates that in these Ni-based systems, spin dephasing in the bulk remains dominant over interfacial or impurity-induced spin-flip scattering.

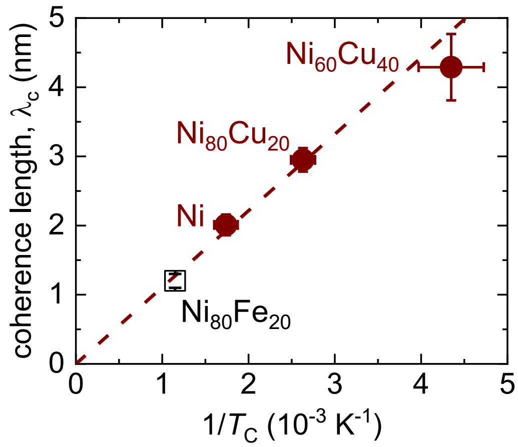

FIG. 4. Transverse spin-current coherence length λ_c plotted against the inverse of the Curie temperature T_C. The data point for $Ni_{80}Fe_{20}$ is from Ref. [13].

The bulk nature of dephasing in these ferromagnets is distinct from prior reports on proximity-magnetized Pd and Pt films, in which the induced magnetic order is confined to a few monolayers at the interface [33,42,43]. It is also noteworthy that $Ni_{60}Cu_{40}$ in our study is essentially on the trend line in Fig. 4, even though its T_C is somewhat below room temperature (see Fig. 2) where the FMR spin pumping measurements were performed. This result suggests that spin-current dephasing may occur even in the bulk of a metal that is "almost" ferromagnetic with fluctuating magnetic order [44]. Alternatively, the fact that λ_c for $Ni_{60}Cu_{40}$ is slightly below the trend line in Fig. 4 may signify that the spin-flip length scale in $Ni_{60}Cu_{40}$ is ≈4 nm, comparable to the dephasing length scale. Though beyond the scope of our present work, the evolution of λ_c for Cu content beyond 40 at.% would be an interesting subject for future experiments.

The above-described measurements of $\Delta\alpha$ (Fig. 3) detect spin absorption in the sink, but they provide no direct insight into what the spin current does inside the sink. We therefore examine the byproduct of the transverse spin current interacting with the magnetization: spin-transfer torque. To this end, we employed the synchrotron-based x-ray ferromagnetic resonance (XFMR) technique [24,45–47] at the Advanced Light Source Beamline 4.0.2 [48], which leverages the element-specificity of x-ray magnetic circular dichroism (XMCD). This XFMR technique can directly detect the magnetization dynamics of a *specific* layer. Moreover, the out-of-plane spin transport here does not involve in-plane net charge transport, hence eliminating ambiguities from coexisting charge-to-spin conversion processes that plague standard electrical spin-torque measurements [49–51].

We conducted XFMR measurements on samples with stack structure MgO(substrate)/Ti(3)/Cu(3)/$Fe_{80}V_{20}$(10)/Ag(5)/Ni(Cu)(5.3)/Ti(3). The (001)-oriented MgO crystal substrate permits high XMCD signals from luminescence yield [48]. As illustrated in Fig. 5(a,b), $Fe_{80}V_{20}$ (instead of $Ni_{80}Fe_{20}$) is the soft low-damping spin source [52,53] for detecting magnetization dynamics via XMCD at the Fe L_3 edge – separately from the Ni L_3 edge for the

Ni(Cu) sink (i.e., Ni or $Ni_{80}Cu_{20}$). The thickness of the Ni(Cu) sink is greater than λ_c to ensure complete spin absorption. Our measurements were performed at a microwave excitation frequency of 4 GHz, using a protocol similar to Ref. [54]. We detected the magnetic oscillations transverse to the in-plane applied field by acquiring the XMCD response vs time. Examples of such time-resolved traces, obtained separately for the FeV source and the Ni(Cu) sink, are shown in Fig. 5(c,d).

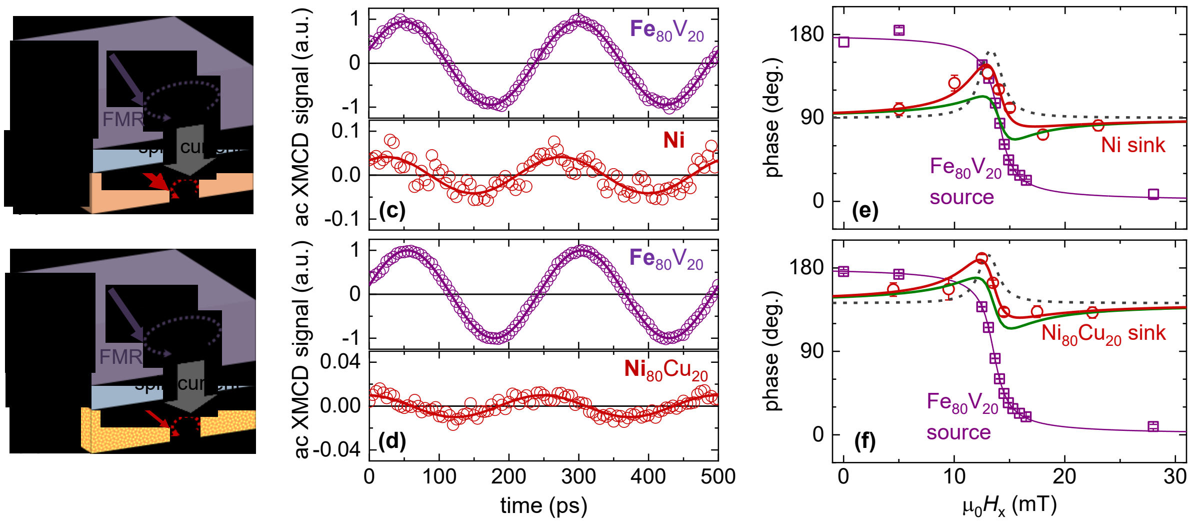

FIG. 5. (a,b) Stack structure for XFMR spin pumping, where the FeV spin source pumps a spin current into the (a) Ni or (b) $Ni_{80}Cu_{20}$ spin sink. (c,d) XMCD response as a function of microwave delay time at the Fe and Ni L_3 edges for the sample with the (c) Ni or (d) $Ni_{80}Cu_{20}$ spin sink. The applied field here is $\mu_0 H_x \approx 14$ mT. (e,f) Field (H_x) dependence of the oscillation phase for the FeV spin source and the (e) Ni or (f) $Ni_{80}Cu_{20}$ spin sink. The solid red curve represents the fit modeling the total torque in the spin sink; the dashed gray curve represents the contribution from the dipolar field torque (with $\beta_{ST} = 0$ in Eq. 2), and the solid green curve represents the contribution from the spin-transfer torque (with $\beta_{dip} = 0$ in Eq. 2).

Figure 5(e,f) summarizes the oscillation phase at several values of in-plane applied field H_x. The FMR of the FeV source is seen as a 180-degree shift in the phase, $\phi^{src} = \mathrm{atan}(\Delta H/(H_x - H_{FMR}^{src}))$, centered at the resonance field $\mu_0 H_{FMR}^{src} \approx 14$ mT with linewidth $\mu_0 \Delta H \approx 0.95$ mT. For the Ni(Cu) sink, we observe a qualitatively distinct shift in the phase ϕ^{snk} around $H_x \approx H_{FMR}^{src}$. We fit ϕ^{snk} vs H_x with the following function [45,55],

$$\phi^{snk} - \phi_0^{snk} = \mathrm{atan}\left(\frac{\beta_{dip}\sin^2\phi^{src} - \beta_{ST}\sin\phi^{src}\cos\phi^{src}}{1 + \beta_{dip}\sin\phi^{src}\cos\phi^{src} + \beta_{ST}\sin^2\phi^{src}}\right), \quad (2)$$

where ϕ_0^{snk} is the baseline phase that depends on the saturation magnetization of the spin sink. The unitless coefficient β_{dip} represents the dipolar field torque (e.g., from the interlayer orange-peel coupling [56] with the precessing source magnetization) normalized by the off-resonant microwave field torque. Similarly, β_{ST} represents the spin-transfer torque (driven by the pumped spin current [24]) normalized by the off-resonant torque. Since the off-resonant torque scales with the magnetization, β_{ST} is also proportional to the efficiency of spin-transfer torque per unit magnetization in the Ni(Cu) sink.

The parameters derived from the fitting with Eq. 2 are summarized in Table I. The comparable values of β_{dip} for the Ni and $Ni_{80}Cu_{20}$ sinks are reasonable because the dipolar- and microwave-field torques scale similarly with the saturation magnetization of the sink. More importantly, β_{ST} also remains the same within experimental uncertainty between Ni and $Ni_{80}Cu_{20}$. We emphasize that β_{ST} is an efficiency metric for the spin-transfer torque *per unit magnetization*. Evidently, the Cu impurities do not diminish this spin-transfer torque efficiency. Our finding confirms that a sizable spin-transfer torque emerges from spin dephasing even in an alloy with a high nonmagnetic impurity content. It also implies that spin-transfer torque can be remarkably robust against electronic momentum scattering by impurities.

	ϕ_0^{snk} (deg.)	β_{dip}	β_{ST}
Ni sink	90 ± 6	1.5 ± 0.5	1.3 ± 0.5
$Ni_{80}Cu_{20}$ sink	142 ± 3	1.0 ± 0.2	1.7 ± 0.3

Table I. Parameters for the fit curves of the total torque for the Ni and $Ni_{80}Cu_{20}$ sinks. ϕ_0^{snk} is the baseline phase; β_{dip} and β_{ST} are coefficients proportional to the dipolar field torque and spin-transfer torque, respectively, normalized by the off-resonant microwave field torque

In summary, we have experimentally investigated the mechanism behind the ultrashort coherence length λ_{c} of transverse spin current in ferromagnetic Ni-based thin films. We find that λ_{c} scales inversely with the exchange strength in the ferromagnets examined here, even those with rather high Cu impurity contents. This central result strongly indicates that dephasing – not scattering – dominates transverse spin-current absorption in these nanometer-thick ferromagnetic metals. This result also highlights the ability to tune λ_{c} by engineering the magnetic exchange. While such tuning was previously explored for *ferri*magnets and antiferromagnets [30,57,58], our study demonstrates that λ_{c} can be extended in *ferro*magnets as well by diluting the magnetic order. We further find that the efficiency of spin-transfer torque in a ferromagnet can remain invariant with its impurity content. Our findings provide crucial insights into transverse spin transport in the "bulk" of nanometer-thick ferromagnets, which may help enhance the performance of spin-torque devices by optimizing the length scale of spin dephasing [29].

Supplementary Material

See supplementary material for additional information on film growth, the estimation of the Curie temperature, and the electrical resistivity of Ni(Cu).

Acknowledgments

Y.L. and S.E. were supported by the Air Force Office of Scientific Research (AFOSR) under Grant No. FA9550-21-1-0365. D.A.S. was supported by the National Science Foundation (NSF) under Grant No. DMR-2003914. This work was made possible by the use of Virginia Tech's Materials Characterization Facility, which is supported by the Institute for Critical Technology and Applied Science, the Macromolecules Innovation Institute, and the Office of the Vice President for Research and Innovation. This research used resources of the Advanced Light Source, a U.S. DOE Office of Science User Facility under Contract No. DE-AC02-05CH11231. S.E. thanks Xin Fan for helpful feedback.

Data Availability

The data that support the findings of this study are available from the corresponding author upon reasonable request.

References

1. I. Žutić, J. Fabian, and S. Das Sarma, "Spintronics: Fundamentals and applications," Rev. Mod. Phys. **76**, 323–410 (2004).

2. W. Han, S. Maekawa, and X.-C. Xie, "Spin current as a probe of quantum materials," Nat. Mater. 1–14 (2019).

3. Q. Shao, P. Li, L. Liu, H. Yang, S. Fukami, A. Razavi, H. Wu, K. Wang, F. Freimuth, Y. Mokrousov, M. D. Stiles, S. Emori, A. Hoffmann, J. Akerman, K. Roy, J.-P. Wang, S.-H. Yang, K. Garellob, and W. Zhang, "Roadmap of spin-orbit torques," IEEE Trans. Magn. 1–1 (2021).

4. D. C. Ralph and M. D. Stiles, "Spin transfer torques," J. Magn. Magn. Mater. **320**, 1190–1216 (2008).

5. A. Brataas, A. D. Kent, and H. Ohno, "Current-induced torques in magnetic materials.," Nat. Mater. **11**, 372–81 (2012).

6. N. Locatelli, V. Cros, and J. Grollier, "Spin-torque building blocks.," Nat. Mater. **13**, 11–20 (2014).

7. A. V. Chumak, A. A. Serga, M. B. Jungfleisch, R. Neb, D. A. Bozhko, V. S. Tiberkevich, and B. Hillebrands, "Direct detection of magnon spin transport by the inverse spin Hall effect," Appl. Phys. Lett. **100**, 82405 (2012).

8. K. An, A. N. Litvinenko, R. Kohno, A. A. Fuad, V. V. Naletov, L. Vila, U. Ebels, G. De Loubens, H. Hurdequint, N. Beaulieu, J. Ben Youssef, N. Vukadinovic, G. E. W. Bauer, A. N. Slavin, V. S. Tiberkevich, and O. Klein, "Coherent long-range transfer of angular momentum between magnon Kittel modes by phonons," Phys. Rev. B **101**, 60407 (2020).

9. M. D. Stiles and A. Zangwill, "Anatomy of spin-transfer torque," Phys. Rev. B **66**, 14407 (2002).

10. M. D. Stiles and J. Miltat, "Spin-Transfer Torque and Dynamics," in *Spin Dynamics in Confined Magnetic Structures III* (Springer Berlin Heidelberg, 2006), pp. 225–308.

11. M. Zwierzycki, Y. Tserkovnyak, P. J. Kelly, A. Brataas, and G. E. W. Bauer, "First-principles study of magnetization relaxation enhancement and spin transfer in thin magnetic films," Phys. Rev. B **71**, 64420 (2005).

12. J. Bass and W. P. Pratt, "Spin-diffusion lengths in metals and alloys, and spin-flipping at metal/metal interfaces: an experimentalist's critical review," J. Phys. Condens. Matter **19**, 183201 (2007).

13. A. Ghosh, S. Auffret, U. Ebels, and W. E. Bailey, "Penetration Depth of Transverse Spin Current in Ultrathin Ferromagnets," Phys. Rev. Lett. **109**, 127202 (2012).

14. Y. Tserkovnyak, A. Brataas, G. E. W. Bauer, and B. I. Halperin, "Nonlocal magnetization dynamics in ferromagnetic heterostructures," Rev. Mod. Phys. **77**, 1375–1421 (2005).

15. S. Blundell, "Ferromagnetism," in *Magnetism in Condensed Matter* (2001), pp. 85–92.

16. M. W. Keller, K. S. Gerace, M. Arora, E. K. Delczeg-Czirjak, J. M. Shaw, and T. J. Silva, "Near-unity spin Hall ratio in N i x C u 1 − x alloys," Phys. Rev. B **99**, 214411 (2019).

17. S. Varotto, M. Cosset-Cheneau, C. Grezes, Y. Fu, P. Warin, A. Brenac, J. F. Jacquot, S. Gambarelli, C. Rinaldi, V. Baltz, J. P. Attane, L. Vila, and P. Noel, "Independence of the Inverse Spin Hall Effect with the Magnetic Phase in Thin NiCu Films," Phys. Rev. Lett. **125**, 267204 (2020).

18. P.-H. Wu, D. Qu, Y.-C. Tu, Y.-Z. Lin, C. L. Chien, and S.-Y. Huang, "Exploiting Spin Fluctuations for Enhanced Pure Spin Current," Phys. Rev. Lett. **128**, 227203 (2022).

19. H. M. Ahmad and D. Greig, "The Electrical Resistivity and Thermopower of Nickel-Copper Alloys," Le J. Phys. Colloq. **35**, C4-223 (1974).

20. R. M. Bozorth, "Temperature and the Curie Point," in *Ferromagnetism* (IEEE, 1978), pp. 713–728.

21. S. Wu, D. A. Smith, P. Nakarmi, A. Rai, M. Clavel, M. K. Hudait, J. Zhao, F. M. Michel, C. Mewes, T. Mewes, and S. Emori, "Room-temperature intrinsic and extrinsic damping in

polycrystalline Fe thin films," Phys. Rev. B **105**, 174408 (2022).

22. J. Beik Mohammadi, J. M. Jones, S. Paul, B. Khodadadi, C. K. A. Mewes, T. Mewes, and C. Kaiser, "Broadband ferromagnetic resonance characterization of anisotropies and relaxation in exchange-biased IrMn/CoFe bilayers," Phys. Rev. B **95**, 64414 (2017).

23. H. J. Zhang, S. Yamamoto, B. Gu, H. Li, M. Maekawa, Y. Fukaya, and A. Kawasuso, "Charge-to-Spin Conversion and Spin Diffusion in Bi/Ag Bilayers Observed by Spin-Polarized Positron Beam," Phys. Rev. Lett. **114**, 166602 (2015).

24. J. Li, L. R. Shelford, P. Shafer, A. Tan, J. X. Deng, P. S. Keatley, C. Hwang, E. Arenholz, G. van der Laan, R. J. Hicken, and Z. Q. Qiu, "Direct Detection of Pure ac Spin Current by X-Ray Pump-Probe Measurements," Phys. Rev. Lett. **117**, 76602 (2016).

25. S. Mizukami, Y. Ando, and T. Miyazaki, "Ferromagnetic resonance linewidth for NM/80NiFe/NM films (NM=Cu, Ta, Pd and Pt)," J. Magn. Magn. Mater. **226–230**, 1640–1642 (2001).

26. S. S. Kalarickal, P. Krivosik, M. Wu, C. E. Patton, M. L. Schneider, P. Kabos, T. J. Silva, and J. P. Nibarger, "Ferromagnetic resonance linewidth in metallic thin films: Comparison of measurement methods," J. Appl. Phys. **99**, 93909 (2006).

27. M. A. W. Schoen, J. Lucassen, H. T. Nembach, T. J. Silva, B. Koopmans, C. H. Back, and J. M. Shaw, "Magnetic properties in ultrathin 3d transition-metal binary alloys. II. Experimental verification of quantitative theories of damping and spin pumping," Phys. Rev. B **95**, 134411 (2017).

28. T. Taniguchi, S. Yakata, H. Imamura, and Y. Ando, "Penetration Depth of Transverse Spin Current in Ferromagnetic Metals," IEEE Trans. Magn. **44**, 2636–2639 (2008).

29. K.-W. Kim, "Spin transparency for the interface of an ultrathin magnet within the spin dephasing length," Phys. Rev. B **99**, 224415 (2019).

30. Y. Lim, B. Khodadadi, J.-F. Li, D. Viehland, A. Manchon, and S. Emori, "Dephasing of transverse spin current in ferrimagnetic alloys," Phys. Rev. B **103**, 24443 (2021).

31. X. Qiu, W. Legrand, P. He, Y. Wu, J. Yu, R. Ramaswamy, A. Manchon, and H. Yang, "Enhanced Spin-Orbit Torque via Modulation of Spin Current Absorption," Phys. Rev. Lett. **117**, 217206 (2016).

32. P. Merodio, A. Ghosh, C. Lemonias, E. Gautier, U. Ebels, M. Chshiev, H. Béa, V. Baltz, and W. E. Bailey, "Penetration depth and absorption mechanisms of spin currents in Ir 20 Mn 80 and Fe 50 Mn 50 polycrystalline films by ferromagnetic resonance and spin pumping," Appl. Phys. Lett. **104**, 32406 (2014).

33. M. Caminale, A. Ghosh, S. Auffret, U. Ebels, K. Ollefs, F. Wilhelm, A. Rogalev, and W. E. Bailey, "Spin pumping damping and magnetic proximity effect in Pd and Pt spin-sink layers," Phys. Rev. B **94**, 14414 (2016).

34. E. Šimánek and B. Heinrich, "Gilbert damping in magnetic multilayers," Phys. Rev. B **67**, 144418 (2003).

35. Y. Ohnuma, H. Adachi, E. Saitoh, and S. Maekawa, "Enhanced dc spin pumping into a fluctuating ferromagnet near T C," Phys. Rev. B **89**, 174417 (2014).

36. B. Khodadadi, J. B. Mohammadi, C. Mewes, T. Mewes, M. Manno, C. Leighton, and C. W. Miller, "Enhanced spin pumping near a magnetic ordering transition," Phys. Rev. B **96**, 54436 (2017).

37. O. Gladii, L. Frangou, G. Forestier, R. L. Seeger, S. Auffret, M. Rubio-Roy, R. Weil, A. Mougin, C. Gomez, W. Jahjah, J.-P. Jay, D. Dekadjevi, D. Spenato, S. Gambarelli, and V. Baltz, "Spin pumping as a generic probe for linear spin fluctuations: demonstration with ferromagnetic and antiferromagnetic orders, metallic and insulating electrical states," Appl. Phys. Express **12**, 23001 (2019).

38. S. Andersson and V. Korenivski, "Exchange coupling and magnetoresistance in CoFe/NiCu/CoFe spin valves near the Curie point of the spacer," J. Appl. Phys. **107**, 09D711 (2010).

39. J. Ryu, M. Kohda, and J. Nitta, "Observation of the D'yakonov-Perel' Spin Relaxation in Single-Crystalline Pt Thin Films," Phys. Rev. Lett. **116**, 256802 (2016).

40. R. Freeman, A. Zholud, Z. Dun, H. Zhou, and S. Urazhdin, "Evidence for Dyakonov-Perel-like Spin Relaxation in Pt," Phys. Rev. Lett. **120**, 67204 (2018).

41. C. T. Boone, J. M. Shaw, H. T. Nembach, and T. J. Silva, "Spin-scattering rates in metallic thin films measured by ferromagnetic resonance damping enhanced by spin-pumping," J. Appl. Phys. **117**, 223910 (2015).

42. P. Omelchenko, E. Girt, and B. Heinrich, "Test of spin pumping into proximity-polarized Pt by in-phase and out-of-phase pumping in Py/Pt/Py," Phys. Rev. B **100**, 144418 (2019).

43. C. Swindells, H. Głowiński, Y. Choi, D. Haskel, P. P. Michałowski, T. Hase, P. Kuświk, and D. Atkinson, "Proximity-induced magnetism and the enhancement of damping in ferromagnetic/heavy metal systems," Appl. Phys. Lett. **119**, 152401 (2021).

44. E. Montoya, B. Heinrich, and E. Girt, "Quantum Well State Induced Oscillation of Pure Spin Currents in Fe / Au / Pd (001) Systems," Phys. Rev. Lett. **113**, 136601 (2014).

45. Q. Li, M. Yang, C. Klewe, P. Shafer, A. T. N'Diaye, D. Hou, T. Y. Wang, N. Gao, E. Saitoh, C. Hwang, R. J. Hicken, J. Li, E. Arenholz, and Z. Q. Qiu, "Coherent ac spin current transmission across an antiferromagnetic CoO insulator," Nat. Commun. **10**, 5265 (2019).

46. D. A. Arena, E. Vescovo, C.-C. Kao, Y. Guan, and W. E. Bailey, "Combined time-resolved x-ray magnetic circular dichroism and ferromagnetic resonance studies of magnetic alloys and multilayers (invited)," J. Appl. Phys. **101**, 09C109 (2007).

47. G. van der Laan, "Time-resolved X-ray detected ferromagnetic resonance of spin

currents," J. Electron Spectros. Relat. Phenomena **220**, 137–146 (2017).

48. C. Klewe, Q. Li, M. Yang, A. T. N'Diaye, D. M. Burn, T. Hesjedal, A. I. Figueroa, C. Hwang, J. Li, R. J. Hicken, P. Shafer, E. Arenholz, G. van der Laan, and Z. Qiu, "Element- and Time-Resolved Measurements of Spin Dynamics Using X-ray Detected Ferromagnetic Resonance," Synchrotron Radiat. News **33**, 12–19 (2020).

49. A. Manchon, J. Železný, I. M. Miron, T. Jungwirth, J. Sinova, A. Thiaville, K. Garello, and P. Gambardella, "Current-induced spin-orbit torques in ferromagnetic and antiferromagnetic systems," Rev. Mod. Phys. **91**, 35004 (2019).

50. A. Davidson, V. P. Amin, W. S. Aljuaid, P. M. Haney, and X. Fan, "Perspectives of electrically generated spin currents in ferromagnetic materials," Phys. Lett. A **384**, 126228 (2020).

51. D. Go, D. Jo, H. W. Lee, M. Kläui, and Y. Mokrousov, "Orbitronics: Orbital currents in solids," Europhys. Lett. **135**, 37001 (2021).

52. M. Arora, E. K. Delczeg-Czirjak, G. Riley, T. J. Silva, H. T. Nembach, O. Eriksson, and J. M. Shaw, "Magnetic Damping in Polycrystalline Thin-Film Fe − V Alloys," Phys. Rev. Appl. **15**, 54031 (2021).

53. D. A. Smith, A. Rai, Y. Lim, T. Q. Hartnett, A. Sapkota, A. Srivastava, C. Mewes, Z. Jiang, M. Clavel, M. K. Hudait, D. D. Viehland, J. J. Heremans, P. V. Balachandran, T. Mewes, and S. Emori, "Magnetic Damping in Epitaxial Iron Alloyed with Vanadium and Aluminum," Phys. Rev. Appl. **14**, 34042 (2020).

54. S. Emori, C. Klewe, J. M. Schmalhorst, J. Krieft, P. Shafer, Y. Lim, D. A. Smith, A. Sapkota, A. Srivastava, C. Mewes, Z. Jiang, B. Khodadadi, H. Elmkharram, J. J. Heremans, E. Arenholz, G. Reiss, and T. Mewes, "Element-Specific Detection of Sub-Nanosecond Spin-Transfer Torque in a Nanomagnet Ensemble," Nano Lett. **20**, 7828–7834 (2020).

55. A. A. Baker, A. I. Figueroa, C. J. Love, S. A. Cavill, T. Hesjedal, and G. van der Laan, "Anisotropic Absorption of Pure Spin Currents," Phys. Rev. Lett. **116**, 47201 (2016).

56. D. A. Arena, E. Vescovo, C.-C. Kao, Y. Guan, and W. E. Bailey, "Weakly coupled motion of individual layers in ferromagnetic resonance," Phys. Rev. B **74**, 64409 (2006).

57. V. Baltz, A. Manchon, M. Tsoi, T. Moriyama, T. Ono, and Y. Tserkovnyak, "Antiferromagnetic spintronics," Rev. Mod. Phys. **90**, 15005 (2018).

58. J. Yu, D. Bang, R. Mishra, R. Ramaswamy, J. H. Oh, H.-J. Park, Y. Jeong, P. Van Thach, D.-K. Lee, G. Go, S.-W. Lee, Y. Wang, S. Shi, X. Qiu, H. Awano, K.-J. Lee, and H. Yang, "Long spin coherence length and bulk-like spin–orbit torque in ferrimagnetic multilayers," Nat. Mater. **18**, 29–34 (2019).